Available online at www.CivileJournal.org

Civil Engineering Journal

(E-ISSN: 2476-3055; ISSN: 2676-6957)

Vol. 11, No. 07, July, 2025

The Influence of Precursor to Activator Ratio and Curing Temperature on Geopolymer Paste with One-Part Method

Ari Widayanti [1*], Januarti J. Ekaputri [2], Iqlima N. Amini [3], Himawan T. B. M. Petrus [4], Anandita Ade Putri [5], Ria A. A. Soemitro [2], Anjas Handayani [6]

[1] *Department of Transportation Engineering, Universitas Negeri Surabaya, Kampus UNESA Ketintang, Surabaya 60231, Indonesia.*

[2] *Department of Civil Engineering, Faculty of Civil, Planning and Geo Engineering, Institut Teknologi Sepuluh Nopember, Kampus ITS, Sukolilo, Surabaya 60111, Indonesia.*

[3] *Department of Civil Engineering, Universitas Negeri Surabaya, Kampus UNESA Ketintang, Surabaya 60231, Indonesia.*

[4] *Department of Chemical Engineering, Faculty of Engineering, Universitas Gadjah Mada, Yogyakarta 55281, Indonesia.*

[5] *Department of Business Management, Faculty of Creative Design and Digital Business, Institut Teknologi Sepuluh Nopember, Kampus ITS, Sukolilo, Surabaya 60111, Indonesia.*

[6] *PT. Semen Indogreen Sentosa (HKSIS), Tegalsari, Surabaya 60265, Indonesia.*

Received 26 December 2024; Revised 18 May 2025; Accepted 23 May 2025; Published 01 July 2025

Abstract

Geopolymer is an eco-friendly material that serves as a sustainable alternative to Portland cement in construction. This binder reduces carbon dioxide emissions from cement production. However, its manufacturing process remains complex and requires professional expertise. This study explores an environmentally friendly cement produced through the "One-Part Method" (or the "just add water" method), which simplifies geopolymer application, making it as user-friendly as Portland cement. However, research on the performance of one-part geopolymers with varying activator contents and curing temperatures remains limited. In this study, Class F fly ash was used as a precursor, combined with a dry activator made from geothermal sludge and sodium hydroxide (NaOH). Two compositions were tested with precursor-to-dry activator ratios of 5:1 (OPG-F5F) and 7:1 (OPG-F7F). The compressive strength was significantly influenced by the Si/Al, Na/Si, Na/Al, and water/solid ratios derived from the precursor and activator. Mechanical properties were analyzed at three curing temperatures: ambient, 40°C, and 60°C. Results showed that OPG-F7F achieved the highest strength at 60°C, reaching 76.1 MPa at 28 days. Mineral analysis before and after steam curing revealed no changes in composition, while morphological analysis indicated that higher temperatures produced a denser geopolymer matrix. These findings demonstrate the strong potential of geopolymer cement as a viable Portland cement replacement using the One-Part Method.

Keywords: Dry Activator; Fly Ash; Geopolymer Paste; One-Part Geopolymer.

1. Introduction

Cement is one of the most widely used construction materials worldwide. However, cement production is a significant source of carbon dioxide (CO_2) emissions, contributing approximately 8% of global carbon emissions [1, 2]. These emissions are primary result from the decomposition of calcium carbonate during the combustion process [3]. To address this environmental challenge, geopolymer materials have emerged as a promising alternative to cement-based concrete due to their lower carbon footprint, high strength, and exceptional durability in extreme conditions [4-6]. The

* Corresponding author: ariwidayanti@unesa.ac.id

http://dx.doi.org/10.28991/CEJ-2025-011-07-014

fundamental difference between Portland cement and geopolymer lies in their reaction mechanisms. The geopolymerization process is influenced by the silica and alumina content, which contribute to the formation of a three-dimensional rigid polymer network, specifically poly(sialate-siloxo) and poly(sialate-disiloxo) [7]. Geopolymers are synthesized using aluminosilicate materials such as fly ash, ground granulated blast furnace slag (GGBFS), and metakaolin, which are activated with an alkaline solution consisting of sodium hydroxide (NaOH) and sodium silicate ($Na_2\ SiO_3$) [8-10]. The conventional geopolymer synthesis process follows a two-part method. First, an alkaline solution is prepared, followed by its mixing with the precursor. This sequential approach increases the overall processing time and poses significant safety concerns due to the use of highly concentrated alkaline solutions, typically ranging from 8 to 16 M NaOH, which are highly corrosive and require careful handling to prevent skin burns [11-13].

An alternative approach, the One-Part method, has been introduced to simplify the geopolymerization process. This method eliminates the need for liquid activators, allowing for a dry-mix formulation that improves handling safety and facilitates large-scale geopolymer concrete production [14-16]. Unlike conventional methods, all components in the One-Part method are prepared in dry form [17]. This method typically utilizes dry powder activators, such as anhydrous sodium metasilicate [18]. However, this material has a high CO_2 emission factor of 1.86 CO_2 -e, making it less environmentally sustainable [19]. Recent studies suggest that alternative activators such as sodium sulfate and sodium carbonate can be used as low-pH activators, though they generally result in lower strength development compared to hydroxide and silicate-based activators [20]. One promising material with a high silica content (>96%) is geothermal sludge, a by-product of silica scale deposits removed during geothermal power plant maintenance [21, 22]. Previous research has explored the use of geothermal sludge as a dry activator, showing that when combined with NaOH and calcined at 400–600°C, sodium metasilicate crystals can form, enhancing its reactivity [17]. Utilizing this material supports circular economy principles by minimizing waste and maximizing resource efficiency in a sustainable manner.

Despite these promising findings, research on geothermal sludge as a geopolymer activator remains limited. Previous studies have shown that geothermal sludge-based activators can achieve compressive strengths ranging from 22.7 MPa to 27.5 MPa, with strength development influenced by the $Na_2\ O/SiO_2$ ratio, calcination temperature, and curing conditions [17, 22]. Additionally, while studies have indicated that an increased $Na_2\ O/SiO_2$ ratio leads to greater N-A-S-H gel formation and improved strength [23], the optimal composition of dry activators and precursors for One-Part Geopolymer remains unclear. Leonard Wijaya et al. [24] also emphasized that the Si/Al ratio significantly influences compressive strength, with an optimal value of 2.0 for conventional geopolymer methods. Further research is needed to determine the ideal ratio for a One-Part Geopolymer using geothermal sludge and fly ash.

Moreover, precursor materials significantly affect the mechanical properties of One-Part Geopolymer. Fly ash is widely used as a silica and alumina source due to its high aluminosilicate content [25, 26]. However, its reactivity is relatively low, requiring a high alkalinity environment to enhance geopolymerization [27]. Studies have also shown that using slag in combination with fly ash can lead to microcrack formation, negatively affecting mechanical performance [28]. Dong et al. [29] found that in One-Part systems activated with sodium metasilicate, the water-to-binder ratio and alkalinity system significantly influence strength development. Additionally, Class F fly ash has been reported to develop compressive strength more slowly due to its lower reactivity [27]. To enhance geopolymerization, steam curing has been proposed as an effective method to improve bond strength and stability. Research has shown that steam curing can significantly increase compressive strength and durability in geopolymer concrete [30-32]. Alnkaa et al. [33] reported that steam curing effectively mitigates shrinkage in geopolymer systems. However, most of these studies have focused on Two-Part Geopolymers, leaving a gap in knowledge regarding its effects on One-Part systems.

Therefore, further investigation into One-Part Geopolymer technology is essential for advancing sustainable construction materials. This study examines the effects of dry activator and precursor composition on the fresh and hardened properties of geopolymer, considering variations in chemical composition and curing temperature. Specifically, it investigates the influence of steam curing on the strength development of fly ash-based One-Part Geopolymer paste. By optimizing precursor and dry activator compositions under different steam curing conditions, this research aims to enhance One-Part Geopolymer formulations as an environmentally friendly alternative to conventional cement. Additionally, the use of geothermal silica and fly ash supports the Sustainable Development Goals (SDGs), particularly Goal 12, which focuses on reducing industrial waste and promoting resource efficiency.

The result and analysis of this article structured as follows: Section 1 discusses the properties of fresh One-Part Geopolymer paste, focusing on normal consistency and setting behavior. Section 2 presents the compressive strength development of One-Part Geopolymer paste under different steam curing conditions. Section 3 compares the mechanical performance of One-Part and Two-Part Geopolymers to evaluate their different process mechanism. Finally, Section 4 provides a microstructural analysis to understand the influence of precursor and activator compositions on geopolymer formation by X-Ray Diffraction (XRD) and Scanning Electron Microscope (SEM) analysis.

2. Materials and Methods

2.1. Materials

One-part geopolymer paste was synthesized using Class F fly ash (FA) sourced from the Suralaya Power Plant, Cilegon, Banten, Indonesia. Figure 1-a shows that the fly ash has a grey color, as analyzed using a Dino-Lite AM4515T5

microscope. Additionally, Figure 1-b presents the scanning electron microscope (SEM) analysis, revealing that the fly ash particles are spherical with a smooth surface. The dry activator (DA) was prepared using geothermal sludge obtained from the Geodipa Dieng Geothermal Power Plant and 98% sodium hydroxide flakes (NF). The chemical composition of these materials, determined by X-ray fluorescence (XRF) analysis, is presented in Table 1. The fly ash consists of 51.61% silicon dioxide (SiO_2) and 24.50% aluminum oxide (Al_2 O_3), whereas the geothermal sludge predominantly contains 75.27% SiO_2 . These results indicate that both materials are highly suitable as aluminosilicate sources for the geopolymerization process.

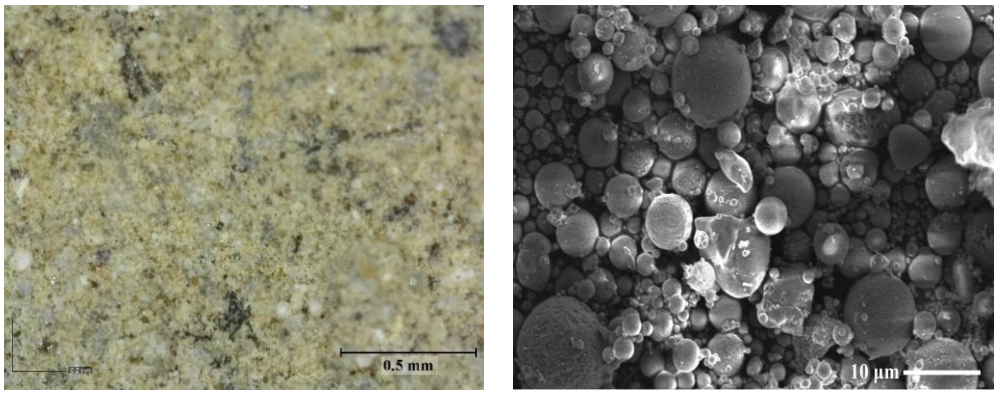

(a) (b)

Figure 1. Fly ash from Suralaya Power Plant (a) Observation by Dino-Lite AM4515T5 (b) Observation by Scanning Electron Microscope (SEM)

Table 1. Chemical and physical properties of raw materials

Chemicals Content (%)	SiO_2	Al_2O_3	Fe_2O_3	CaO	MgO	Na_2O	K_2O	SO_3	Others	LOI	%Fineness (retained)
Fly Ash (FA)	51.61	24.50	7.59	6.39	2.63	2.38	0.77	0.96	1.43	1.37	14.90
Geothermal Sludge (GS)	75.27	0.14	1.92	0.13	0.13	2.55	1.05	0.64	5.27	12.9	-
Dry Activator	-	-	-	-	-	-	-	-	-	-	72.60

2.2. Method

2.2.1. Preparation of dry activator (DA)

The dry activator preparation process is illustrated in Figure 2. Geothermal sludge (GS) was first purified by soaking it in boiled distilled water at a 4:1 ratio to remove impurities, followed by drying at 110°C for 24 hours. The dried GS was then mixed with sodium hydroxide (NaOH) flakes in a 1:1 ratio and further dried at 200°C to eliminate residual moisture. Next, the mixture underwent calcination at 400°C for 10 hours, resulting in material agglomeration. To ensure homogeneity, the calcined product was ground using a dry mill and stored in a high-density polyethylene (HDPE) bottle to prevent moisture absorption.

Figure 2. Workflow of dry activator preparation

2.2.2. Specimen Preparation

The specimens were prepared using two geopolymer synthesis methods: the One-Part method (OPG) and the Two-Part method (GC). The material proportions are presented in Table 2, while the specimen preparation process is illustrated in Figure 3. In the One-Part method, the precursor was first mixed with the dry activator (DA) and homogenized using a dry mill to form geopolymer cement. Water was then added, with its content determined through a normal consistency test. The precursor-to-DA (P/DA) ratios used were 5:1 and 7:1. The mixture was cast into cylindrical molds with a diameter of 2 cm and a height of 4 cm. Curing was conducted under three conditions: (1) ambient temperature, (2) steam curing at 40°C, and (3) steam curing at 60°C for 24 hours, followed by storage in moist conditions until testing. For comparison, conventional geopolymer paste was produced using the Two-Part method while maintaining identical Si/Al, Na/Si, Ca/Si, Ca/Al, and Na/Al ratios.

Table 2. Detail of mix proportion One-Part & Two-Part Geopolymer

Mix	Fly Ash (%)	DA (%)	Fly Ash: DA	Alkaline Solution (%)	NaOH: Na_2SiO_3
OPG-F5F	70.9	14.2	5:1	-	-
OPG-F7F	73.0	10.4	7:1	-	-
GC-F5F	67.0	-	-	33.0	1:1

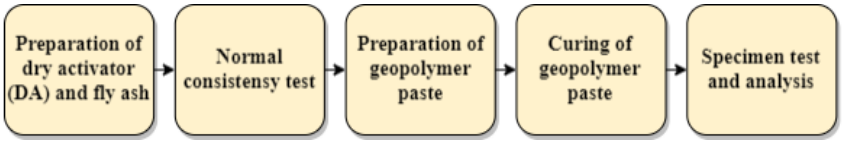

Figure 3. Flow chart of proposed methodology

2.2.3. Test Parameter

The raw materials were analyzed using X-Ray Fluorescence (XRF). In the fresh condition, the geopolymer paste was tested for normal consistency and setting time following ASTM C187 and ASTM C191. In the hardened state, compressive strength tests were conducted using a universal testing machine at 7, 14, and 28 days. The chemical composition of the geopolymer paste was also analyzed using XRF from the raw material to determine the Si/Al, Na/Si, Ca/Si, Ca/Al, and Na/Al ratios. These atomic ratios were calculated based on the total atomic molarity of the raw materials, as presented in Table 3. Additionally, mineralogical analysis was performed using X-Ray Diffraction (XRD), and the microstructural characteristics were examined through Scanning Electron Microscopy (SEM).

Table 3. Calculation of atom molarity

Chemical Reaction	Total atom molarity $\left(n = \frac{m}{Mr}\right)$	Atomic ratio (A/B)
$Na_2O \rightarrow 2Na + \frac{1}{2}O_2$	Total mol Na	$\frac{Total\ mol\ A}{Total\ mol\ B}$
$SiO_2 \rightarrow Si + O_2$	Total mol Si	
$Al_2O_3 \rightarrow 2Al + \frac{3}{2}O_2$	Total mol Al	
$Fe_2O_3 \rightarrow 2Fe + \frac{3}{2}O_2$	Total mol Fe	
$CaO \rightarrow Ca + \frac{1}{2}O_2$	Total mol Ca	

3. Results and Discussion

3.1. Properties of Fresh One Part Geopolymer Paste

3.1.1. Normal Consistency

The effect of precursor content is presented in Figure 4. It can be observed that water content increases linearly with an increase in precursor content. The water content in OPG-F7F increased by 13.94% compared to OPG-F5F. A decrease in dry activator content resulted in a higher water demand for fly ash. According to Karim et al. [34] and Cheerarot & Jaturapitakkul [35], this phenomenon occurs due to the high porosity of fly ash, which allows it to absorb more water. In the One-Part method, the precursor composition significantly influences the water-to-binder (w/b) ratio, which, in

turn, affects the workability of the mixture. In geopolymer reactions, water does not participate in the geopolymerization process but serves solely as a reaction medium [36, 37]. Therefore, in the OPG-F7F composition, which contains a higher proportion of fly ash, more water is required to facilitate the distribution of the activator across the fly ash surface and to ensure sufficient dissolution.

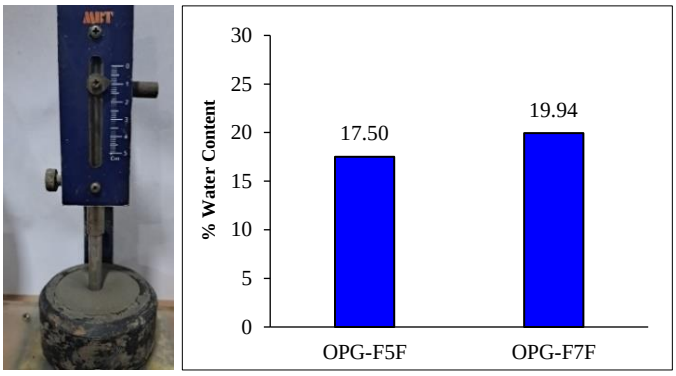

Figure 4. The result of normal consistency of one-part geopolymer paste

3.1.2. Setting Time

Figure 5 illustrates the effect of the precursor-to-dry activator (P/DA) ratio and precursor type on the setting time. The results indicate that an increase in precursor content accelerates the setting time. The final setting time of OPG-F5F decreased by 33% when the fly ash content increased, and the dry activator content decreased (OPG-F7F). In the One-Part geopolymer system, water absorption is primarily influenced by fly ash. This phenomenon is attributed to the differences in particle size between fly ash and the dry activator. As shown in Table 1, fly ash has a finer particle size than the dry activator. Chemically, this is further explained by the Si/Al ratio presented in Table 4, where the Si/Al ratio decreases from 2.05 in OPG-F5F to 1.98 in OPG-F7F. An increase in silica content in the system results in a longer setting time [38]. Silva et al. [7] reported that the condensation reaction forming Si–O–Si bonds occurs more slowly than that forming Si–O–Al bonds. Consequently, a higher silica content prolongs the setting time.

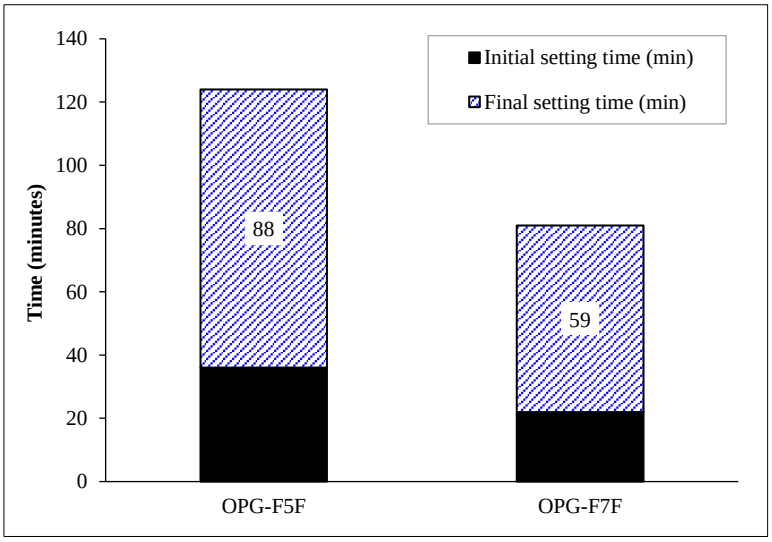

Figure 5. Setting time of one-part geopolymer

3.2. Compressive Strength of One Part Geopolymer Paste

3.2.1. The Effect of Chemical Content

The geopolymerization reaction is highly influenced by the chemical composition of the raw materials. Davidovits [39] explained that geopolymers are synthesized through a geopolymerization process involving the chemical reaction between silica and alumina, forming amorphous Si–O–Al polymer bonds. Consequently, silica and alumina play a crucial role in determining the strength of geopolymers. Table 4 presents the Si/Al ratios for OPG-F5F and OPG-F7F. The results indicate that increasing the precursor-to-dry activator (P/DA) ratio lowers the Si/Al ratio. The dry activator, which contains geothermal sludge, significantly contributes to the silica content in the mixture. A lower dry activator (DA) content leads to reduced silica availability. Similarly, the Na/Si and Na/Al ratios also decrease with a reduction in DA content. These ratios are critical, as sodium (Na) acts as an activator for silica and alumina during geopolymerization.

Figure 6 illustrates the relationship between compressive strength and the Si/Al, Na/Si, and Na/Al ratios. The results show that a decrease in the Si/Al, Na/Si, and Na/Al ratios enhances the compressive strength of the geopolymer paste. Consistent with the setting time analysis, a higher silica content prolongs binding time, corresponding to an increased Si/Al ratio, which, in turn, reduces compressive strength (Figure 6-a). As the Si/Al ratio increased by 3.5%, the compressive strength decreased by 42%. Similar findings were reported by Wang et al. [40] and Lee et al. [41], who observed that an increase in the Si/Al ratio leads to a decline in compressive strength. This effect is attributed to an excessive silicate activator, which hinders ion migration and reduces compressive strength development. de Jong & Brown [42] explained that Si–O–Si bonds are inherently stronger than Si–O–Al and Al–O–Al bonds. However, the compressive strength results indicate that a higher silica content in OPG-F5F does not yield superior strength compared to OPG-F7F, which contains less silica. Duxson et al. [43] suggested that although a greater number of Si–O–Si bonds are formed, which are theoretically stronger, the resulting microstructure may be less homogeneous and less dense. This occurs because the gel network may fail to reorganize completely, leading to lower compressive strength despite an increased Si/Al ratio. These findings suggest that the Si/Al ratio significantly influences compressive strength. Liu et al. [44] further emphasized that the optimal Si/Al ratio varies depending on the physical and chemical characteristics of the precursor materials. Therefore, additional investigation is required to determine the optimal Si/Al ratio for one-part geopolymer synthesis.

Table 4. Si/Al, Na/Si, Ca/Si, Ca/Al, Na/Al and Water/Solid of one-part geopolymer specimen

Code	Si/Al	Na/Si	Ca/Si	Ca/Al	Na/Al	Water/Solid
OPG-F5F	2.05	0.41	0.12	0.24	0.85	0.18
OPG-F7F	1.98	0.33	0.12	0.24	0.65	0.20

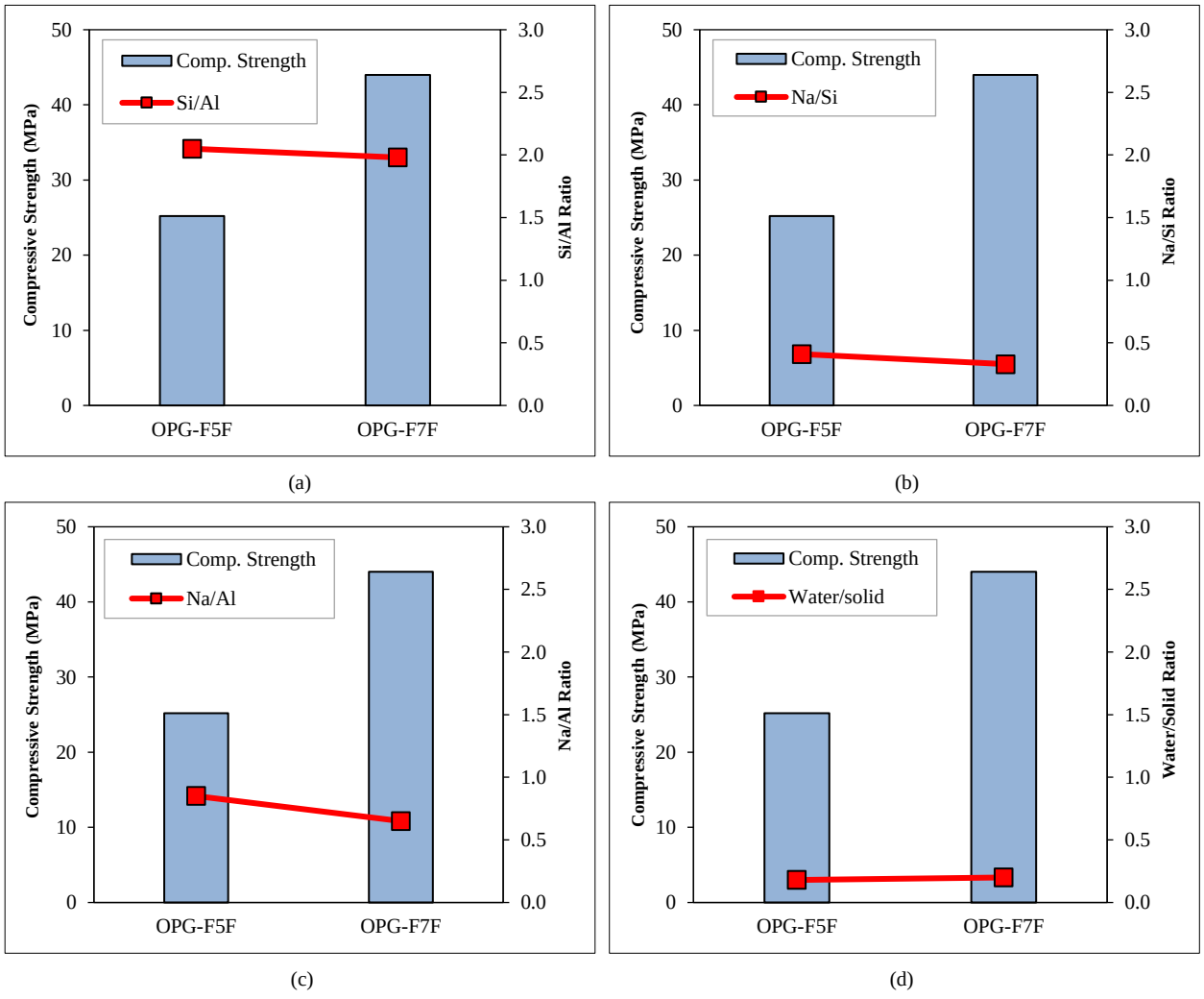

Figure 6. The effect of chemical ratio on geopolymer paste compressive strength (a) Si/Al (b) Na/Si (c) Na/Al and (d) Water/solid

The increase in the P/DA ratio also affects sodium (Na) content, which originates from the dry activator. A higher fly ash content in the geopolymer paste results in a lower sodium concentration, subsequently reducing the Na/Si and

Na/Al ratios. In this study, a decrease in the Na/Si and Na/Al ratios led to an increase in compressive strength (Figures 6-b and 6-c). In contrast, in two-part geopolymers, a reduction in sodium concentration generally lowers compressive strength, as an insufficient NaOH concentration fails to optimally trigger geopolymerization [45, 46]. This highlights a fundamental difference between two-part and one-part geopolymers. In a two-part system, sodium hydroxide concentration is the dominant factor influencing strength development. However, in a one-part system, water plays a crucial role. Since water is added last in one-part geopolymer synthesis, it serves as both an ion transport medium for silica and alumina activation and is also absorbed by fly ash. In the formation of geopolymerization reactions, water plays a very important role [47, 48]. The results of the normal consistency test (Figure 4) indicate that OPG-F5F contains less water than OPG-F7F. Table 4 and Figure 6-d further show that the water-to-solid ratio of OPG-F7F is higher than that of OPG-F5F. These findings suggest that in OPG-F7F, more water is absorbed by the activator, leading to a more effective reaction with silica and alumina. Consequently, the activator functions more efficiently, enhancing compressive strength development. Ma et al. [49] also found similar findings, indicating that an adequate water-to-solid ratio facilitates the dissolution of silica and alumina, thereby enhancing geopolymer gel formation. Conversely, an excessively low water-to-solid ratio can lead to crystal precipitation, which inhibits further dissolution.

3.2.2. The Effect of Curing Temperature

The compressive strength of OPG paste under different curing temperatures is presented in Figure 7. The results indicate that increasing the steam curing temperature has a linear effect on enhancing compressive strength across all variations. Significant differences were observed, particularly in the rate of strength development, with the most notable changes occurring at an early age (7 days). At 7 days and a curing temperature of 40°C, the compressive strength of OPG-F5F increased by 68%, whereas OPG-F7F showed an increase of 24%. When the curing temperature was raised to 60°C, the compressive strength of OPG-F5F nearly doubled, increasing by 104%, while OPG-F7F exhibited an 80% increase. Furthermore, at 28 days, steam curing at 40°C led to a 40% increase in compressive strength, while curing at 60°C resulted in an approximately 50% increase. Figure 7b presents the compressive strength results for OPG-F7F under different curing temperatures, showing a 15.68% increase under steam curing at 40°C and a 73% increase at 60°C. The rate of compressive strength development at 7, 14, and 28 days was generally slower in OPG-F5F compared to OPG-F7F.

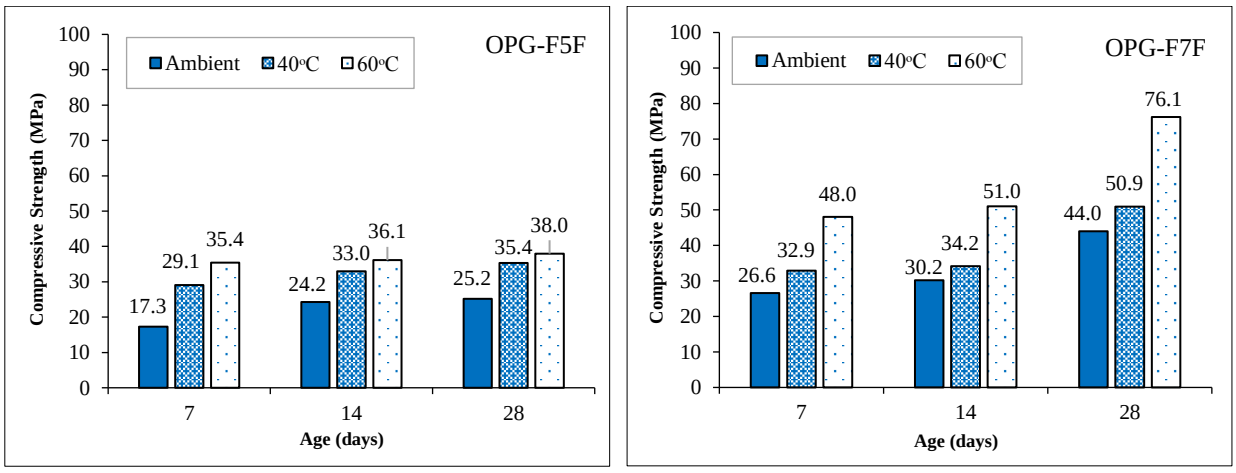

(a) (b)

Figure 7. The effect of curing temperature on compressive strength of one-part geopolymer paste (a)OPG-F5F (b) OPG-F7F

Several studies have demonstrated that steam curing significantly enhances early-age compressive strength [50-52]. This effect occurs because the alkali activator cannot fully activate fly ash due to its low reactivity, particularly at ambient temperatures [27, 53]. Additionally, high temperature curing effectively accelerates the geopolymerization reaction [54-56]. Sajan et al. [57] explained that elevated temperatures increase the reactivity of Na^+ and OH^- ions, resulting in a denser microstructure. High temperatures also facilitate the transformation of the geopolymerization reaction from a 2D chain structure into a more stable 3D network with stronger bonds [57]. Wu et al. [58], reported that steam curing enhances the dissolution of silica and alumina in fly ash by providing thermal energy to break Si–O and Al–O bonds. Similarly, Petrus et al. [59] confirmed that steam treatment promotes the dissolution of silica and alumina, further improving the geopolymerization process. In the OPG-F7F composition, the dissolution of silica and alumina using the steam curing method is more effective than in OPG-F5F, as evidenced by the higher strength development. This result aligns with the previous explanation that water plays a crucial role in strength development. Additionally, the higher fly ash content in the OPG-F7F composition significantly contributes to strength enhancement. Liu et al. [60] stated that the dissolution of silica and alumina in fly ash is highly effective when using steam curing.

3.2.3. The Effect of Precursor and Dry Activator Ratio on Different Curing Temperature

The development of compressive strength with different precursor-to-dry activator (P/DA) ratios is presented in Figures 8-a to 8-c. The results indicate that a higher dry activator content (OPG-F5F) reduces compressive strength by 42% at 28 days compared to OPG-F7F under ambient conditions. Under ambient curing, the compressive strength of OPG-F5F exhibited more stable growth from 14 to 28 days than OPG-F7F. This stability is attributed to a weaker geopolymerization reaction in the OPG-F5F system. The limited reaction at ambient temperature is evident from the significant strength increase when steam curing is applied at 40°C and 60°C. The primary reason for the inefficient geopolymerization in OPG-F5F is insufficient water content, which reduces its interaction with the alkali activator. Water plays a crucial role as an ion transport medium for silica and alumina activation during geopolymerization [47, 48]. Even at elevated curing temperatures, the geopolymerization process remains suboptimal in the absence of adequate water.

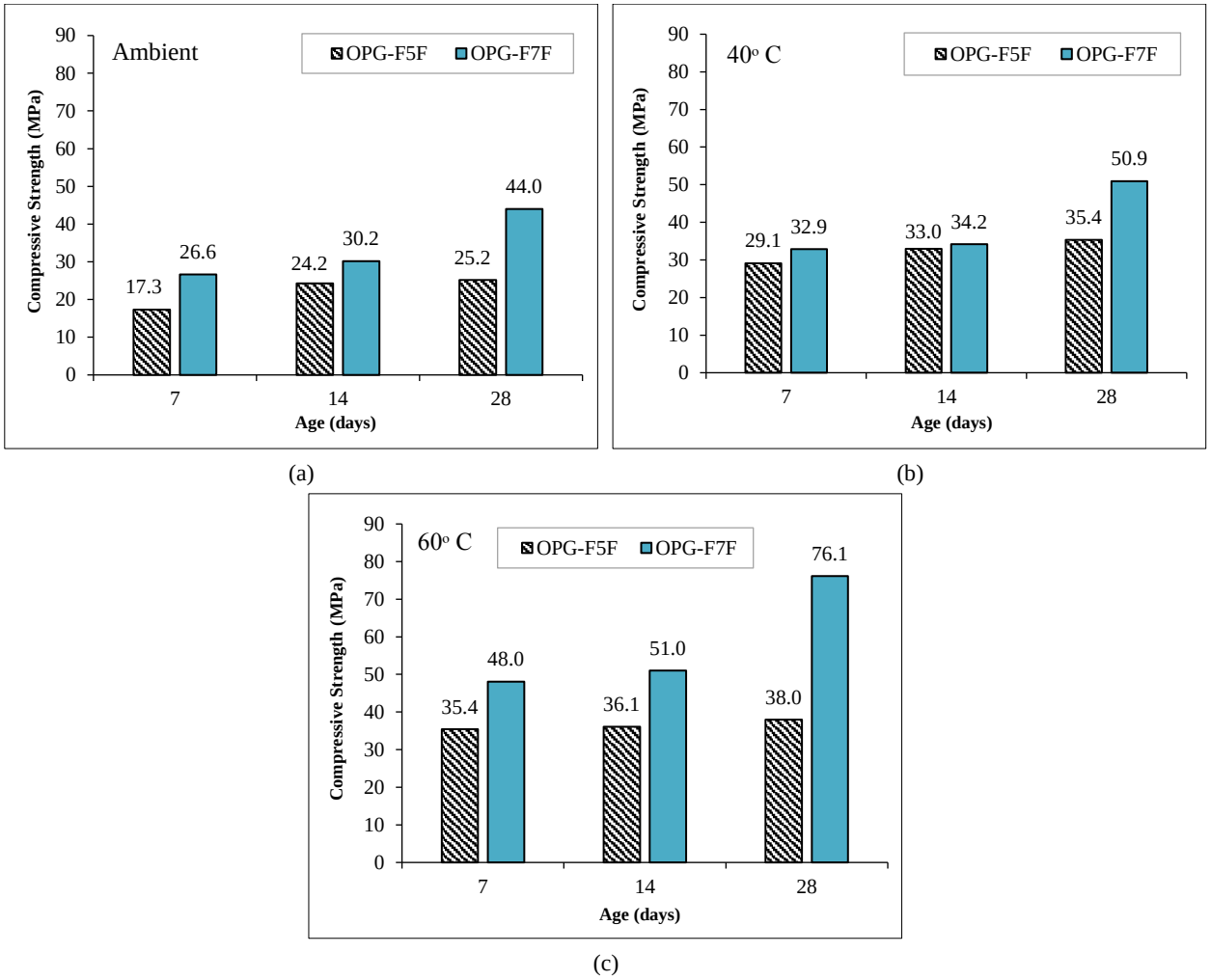

Figure 8. The effect of precursor and dry activator ratio on different curing temperature (a) ambient, (b) 40°C and (c) 60°C

Table 4 shows that the Na/Si and Si/Al ratios decrease as the P/DA ratio increases, correlating with higher compressive strength. A higher Na/Si ratio indicates an excess of sodium in the system. Figure 9 presents surface observations of OPG-F5F and OPG-F7F specimens, captured using a Dino-Lite microscope at 50x and 225x magnifications. In the OPG-F5F specimen, salt accumulation and surface cracks were observed, likely due to excessive sodium content. Previous studies have shown that an excess of sodium in a geopolymer system inhibits the geopolymerization process and promotes the formation of sodium carbonate minerals upon reaction with CO_2 [61-63]. This phenomenon, known as efflorescence, is characterized by salt deposits, as illustrated in Figure 9-b. The impact of efflorescence on compressive strength remains inconclusive, as crystallization can either densify the pore structure potentially improving strength or weaken the matrix if excessive, making efflorescence generally undesirable for geopolymer materials [64]. Additionally, surface cracks were observed in the OPG-F5F specimen, likely caused by self-desiccation due to insufficient water content in the mixture. Sodium promotes water absorption, forming hydrated sodium compounds that contribute to drying shrinkage [65]. This phenomenon is also explained by Hanumananaik & Subramaniam [66], who reported that excessive sodium in geopolymer systems can lead to shrinkage, as sodium acts as a filler that reduces pore size.

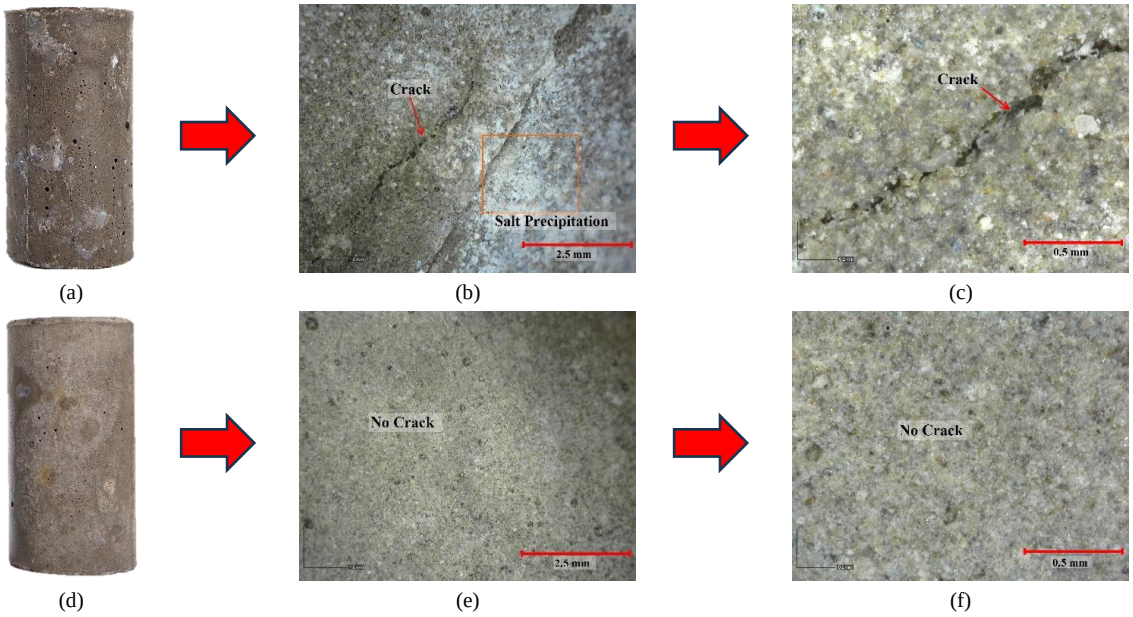

Figure 9. Surface appearance of One-Part Geopolymer Paste (a) OPG-F5F after casting (b) Salt precipitation analysis of OPG-F5F (c) Surface crack analysis of OPG-F5F (d) OPG-F7F after casting (e) Surface analysis of OPG-F7F (no salt precipitation observed) (f) Surface crack analysis of OPG-F7F (no surface cracks observed).

Petrus et al. [17] also studied mortar using a dry activator composed of geothermal silica and NaOH with a fly ash-to-dry activator ratio of 4:1. The compressive strength obtained was 27.5 MPa at a Na_2 O/SiO_2 ratio of 0.692, influenced by a well-balanced availability of Na^+ ions and reactive silica, which facilitated the formation of a denser and stronger geopolymer structure. This indicates that further research is needed to determine the optimal dry activator-to-silica ratio to achieve the appropriate sodium composition for silica reaction. Moreover, the Si/Al ratio significantly influences the strength of one-part geopolymer paste. A higher Si/Al ratio is directly associated with slower setting times, as excess silica prolongs compressive strength development. Petrus et al. [17] also reported similar findings, indicating that a reduction in silica and sodium content enhances compressive strength.

3.3. Comparison Between One-Part Geopolymer and Two Part Geopolymer

Figure 10 compares the compressive strength of geopolymers synthesized using the One-Part and Two-Part methods. The results show that despite having identical Si/Al, Na/Si, Ca/Si, Ca/Al, and Na/Al ratios, differences in compressive strength were observed. Specifically, the Two-Part method for the GC-F5F variation achieved 48% higher compressive strength than the One-Part method for the OPG-F5F variation. The strength development of geopolymers is influenced by both the raw materials and the alkaline activator solution, which play a crucial role in the formation of geopolymerization products, particularly N-A-S-H gel [67, 68]. According to previous studies [69, 70], the primary difference between One-Part and Two-Part geopolymers lies in their preparation methods. In the Two-Part system, the solid activator (Na_2 SiO_3 and NaOH) first dissolves through an exothermic reaction before reacting with the precursor. In contrast, One-Part geopolymers undergo both processes simultaneously, leading to differences in heat release and reaction progression during geopolymerization. As a result, strength development in the One-Part method is slower than in the Two-Part method.

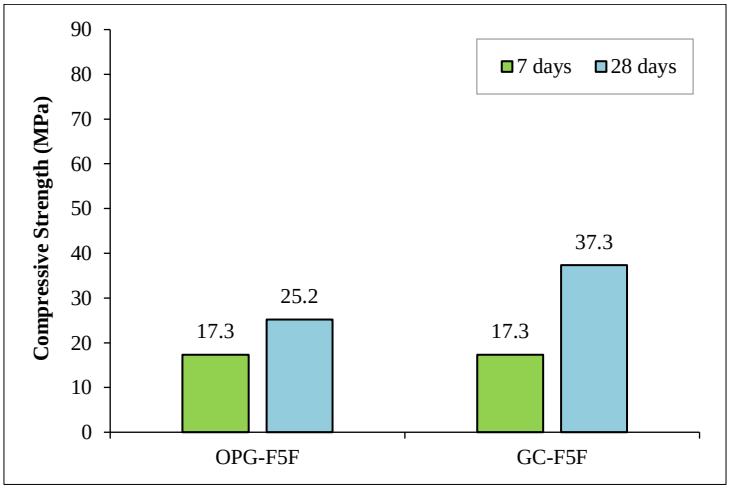

Figure 10. Strength comparison of One-Part and Two-Part geopolymer paste

Tables 4 and 5 show that the most significant difference between these methods is the water-to-solid ratio. In the Two-Part method, the water-to-solid ratio is higher than in the One-Part method. In the Two-Part system, water originates from the alkaline solution, whereas in the One-Part system, water is added during mixing. In the Two-Part method, water does not actively participate in the geopolymerization reaction but serves as a medium for sodium transport, facilitating the dissolution of silica and alumina from the precursor [71]. Conversely, in the One-Part method, the added water is absorbed by both the activator and fly ash, as both materials require water for the reaction. Sodium needs water to facilitate geopolymer structure formation. Further research is needed to determine the optimal water content required for both the alkaline activator and precursor in the One-Part system. Differences in the water-to-solid ratio also affect the workability of the mixtures. In the GC-F5F specimen, the higher water content results in a more fluid mixture compared to OPG-F5F. The variation in consistency between these mixtures influences their solidification behavior, ultimately leading to differences in compressive strength. Konduru & Karthiyaini [72], also emphasized that the initial consistency of the geopolymer mix is crucial, as it determines fresh-state characteristics, directly influencing the solidification process and final strength.

Table 5. Si/Al, Na/Si, Ca/Si, Ca/Al, Na/Al and Water/Solid of F5F specimen

Code	Si/Al	Na/Si	Ca/Si	Ca/Al	Na/Al	Water/Solid	NaOH Molarity
GC-F5F	2.05	0.41	0.12	0.24	0.85	0.25	11.4 M

3.4. Microstructural Analysis

3.4.1. X-Ray Diffraction (XRD) Analysis

Mineral analysis was conducted using X-ray Diffraction (XRD), and the results are presented in Figure 11. The dominant minerals identified in the specimens were Quartz (SiO_2), Mullite ($3Al_2O_3 \cdot 2SiO_2$), Magnetite (Fe_3O_4), and geopolymerization products (N-A-S-H). Quartz and Mullite originated from fly ash [73]. The geopolymerization products consisted of aluminosilicate minerals, including Analcime, Natrolite, Sodalite, Albite, and Cancrinite. Variations in the precursor-to-dry activator ratio did not significantly affect the types of minerals identified by XRD; however, they influenced the peak intensity variations. In the OPG-F7F variation, the Quartz peak intensity increased, likely due to the contribution of unreacted fly ash.

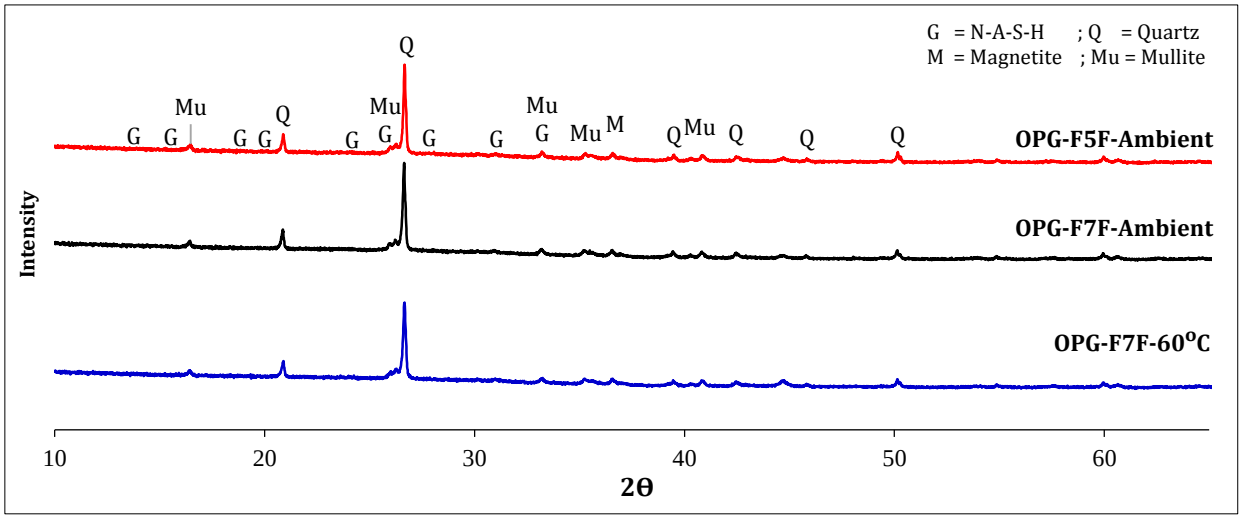

Figure 11. X-Ray Diffraction (XRD) pattern of one-part geopolymer paste

The overall XRD patterns of specimens cured at ambient and steam curing conditions (60°C) remained similar, indicating that heat treatment did not alter the mineral phases formed in the one-part geopolymer system. Similar findings have been reported in previous studies [74-76]. However, a significant reduction in peak intensity was observed in the OPG-F7F variation after steam curing at 60°C, which is attributed to an increase in the amorphous content from 90.38% to 91.45% at higher curing temperatures. A similar trend was reported by Christidis et al. [77]. Chouksey et al [74] explained that this phenomenon results from a decrease in oxide minerals within the geopolymer system. This suggests an enhancement of the geopolymerization reaction under steam curing conditions at 60°C. These findings align with the observed increase in compressive strength of the OPG-F7F variation due to steam curing, as shown in Figure 7-b.

3.4.2. Scanning Electron Microscope (SEM) Analysis

The SEM images of OPG samples (OPG-F7F and OPG-F7FL) under different curing temperatures are shown in Figure 12. This study compares the microstructural morphology of geopolymer samples. In the OPG-F7F specimen cured at room temperature (Figure 12-a), the microstructure appears more porous, with numerous microcracks observed. EDS mapping confirms that the matrix consists of Na, Si, and Al elements, forming sodium aluminosilicate hydrate (N-A-S-H), the primary geopolymerization product. Khale & Chaudhary [78], explained that microcracks result from water loss, leading to shrinkage. Additionally, the exothermic reaction between NaOH and water during the initial mixing stage contributes to shrinkage due to thermal-induced water evaporation. This phenomenon has also been reported by Wang et al. [79] and Ma et al. [80], who noted that the one-part geopolymerization method generates heat during the initial mixing phase.

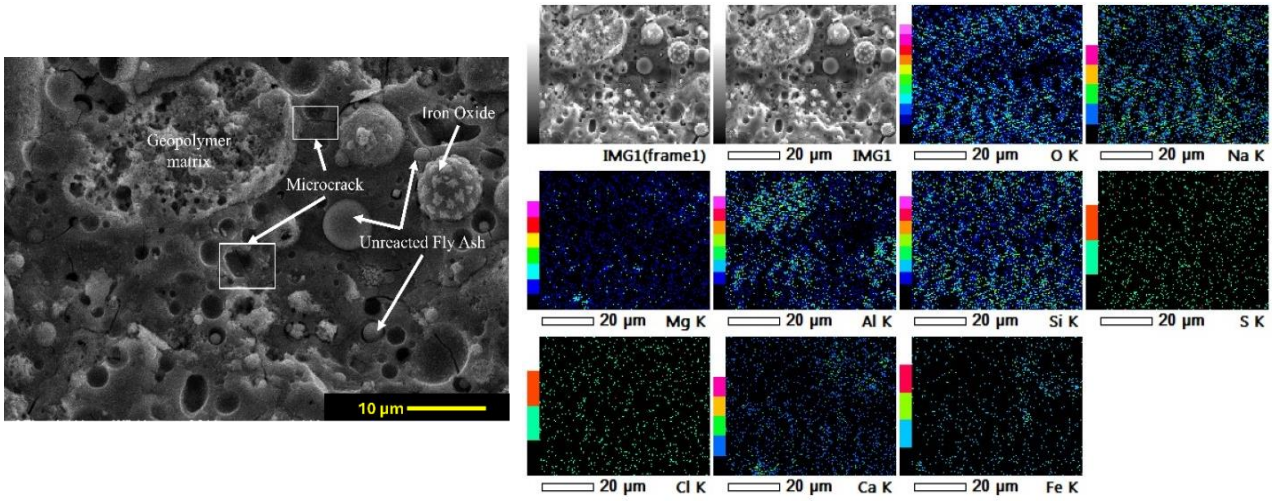

(a)

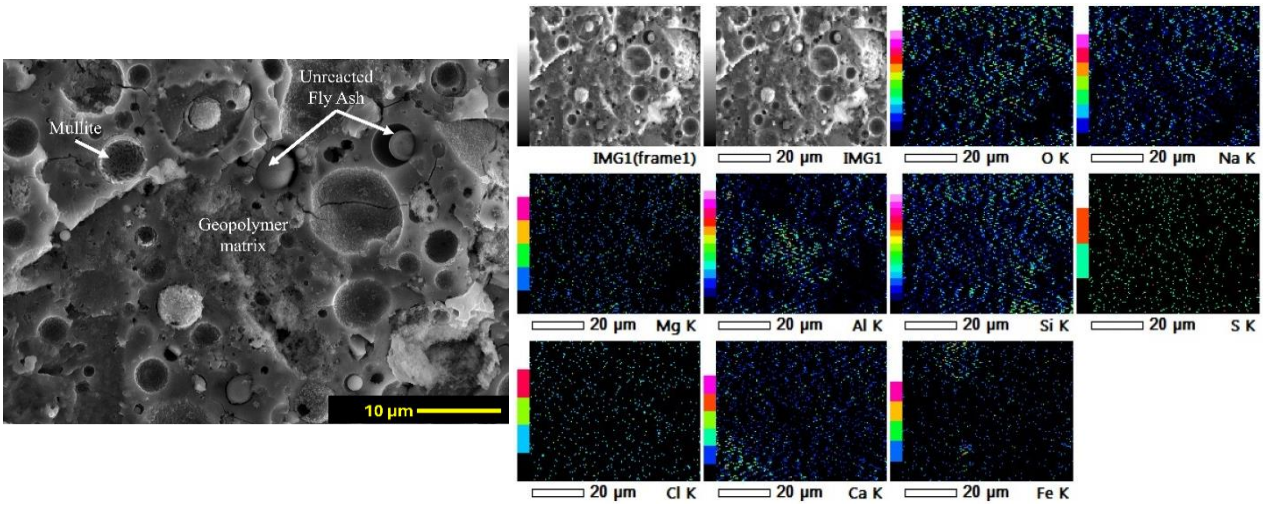

(b)

Figure 12. Scanning Electron Microscope (SEM) analysis (a) OPG-F7F at ambient temperature (b) OPG-F7F steam at 60^{o}C

A significant difference in morphology is observed in the OPG-F7F specimen after steam curing at 60°C. As shown in Figure 12-b, the microstructure of the steam-cured specimen is notably denser than that of the room-temperature-cured specimen. EDS mapping analysis (Figure 12(b)) indicates no significant changes in the elemental composition of the matrix due to temperature variation. This result aligns with the XRD analysis, which shows that the mineral phases remain unchanged at elevated temperatures. However, a greater proportion of fly ash particles react during steam curing compared to room-temperature curing [30, 81, 82]. The additional thermal energy enhances the dissolution of fly ash particles, accelerating the geopolymerization reaction and resulting in a denser microstructure with fewer microcracks. Furthermore, the steam curing process provides a humid environment, reducing rapid water loss and minimizing crack formation [33, 83].

4. Conclusions

This study examined the effects of the precursor-to-dry activator ratio and curing temperature on geopolymer paste synthesized using the One-Part Method. The following conclusions were drawn:

- The precursor-to-dry activator ratio significantly influences the water demand of the mixture. A lower activator content requires a higher water addition, which enhances the dispersion of the activator on the fly ash surface. Additionally, this ratio affects the setting time, which is governed by the Si/Al ratio of the mixture.
- Increasing the precursor-to-dry activator ratio reduces the Si/Al, Na/Al, and Na/Si ratios while increasing the water-to-solid ratio. A 3.5% reduction in the Si/Al ratio leads to a 42% increase in compressive strength. This is attributed to the excess silicate activator limiting ion migration, thereby hindering strength development. Similarly, the Na/Al and Na/Si ratios influence the alkali hydroxide concentration in the One-Part system. However, the key parameter is the water-to-solid ratio, which plays a crucial role in alkali distribution and the dissolution of silica and alumina from fly ash.
- Steam curing significantly enhances the early-age compressive strength of the geopolymer. At 7 days, compressive strength increased by 104% for OPG-F5F and 80% for OPG-F7F when cured at 60°C. The low reactivity of fly ash necessitates higher curing temperatures, as the alkali activator cannot fully react with fly ash at lower temperatures.
- A higher alkali activator content does not necessarily result in greater compressive strength for OPG-F5F compared to OPG-F7F. At ambient temperature, as well as after steam curing at 40°C and 60°C, OPG-F7F exhibited a greater increase in strength than OPG-F5F. This is due to insufficient water content in OPG-F5F, which restricts alkali transport and hinders silica and alumina activation. Increasing the curing temperature alone is insufficient to achieve optimal strength. Further research is needed to investigate the role of water in geopolymer paste preparation using the One-Part Method.
- XRD analysis revealed that increasing the curing temperature to 60°C in OPG-F7F did not alter the mineral composition. However, a reduction in peak intensity after steam curing indicates a decrease in oxide minerals. The steam curing process resulted in a denser microstructure compared to ambient curing, as the additional thermal energy enhanced the dissolution of silica and alumina from fly ash.

5. Declarations

5.1. Author Contributions

Conceptualization, A.W., J.E.J., and H.T.B.M.P.; methodology, J.E.J. and H.T.B.M.P.; software, I.N.A.; validation, A.W., J.E.J., and R.A.A.S.; formal analysis, J.E.J. and I.N.A.; investigation, A.W. and I.N.A.; resources, J.E.J. and H.T.B.M.P; data curation, A.W.; writing—original draft preparation, A.W. and I.N.A.; writing—review and editing, J.E.J., R.A.A.S., and A.A.P.; visualization, I.N.A. and A.A.P.; supervision, J.E.J. and H.T.B.M.P.; project administration, A.W. and I.N.A.; funding acquisition, A.W. and A.H. All authors have read and agreed to the published version of the manuscript.

5.2. Data Availability Statement

The data presented in this study are available in the article.

5.3. Funding

This research was funded by Universitas Negeri Surabaya, under Indonesian Collaborative Research Scheme with contract number 493.UN38/HK/2024.

5.4. Acknowledgements

The authors gratefully acknowledge to the Rector of Universitas Negeri Surabaya, the Head of the Institute for Research and Community Service of Universitas Negeri Surabaya. And, to partners PT. Semen Indogreen Sentosa (HKSIS), Suralaya Power Plant, Institut Teknologi Sepuluh Nopember and UGM, who played a role in making this research did.

5.5. Conflicts of Interest

The authors declare no conflict of interest.

6. References

[1] Liu, Z., Ciais, P., Deng, Z., Davis, S. J., Zheng, B., Wang, Y., Cui, D., Zhu, B., Dou, X., Ke, P., Sun, T., Guo, R., Zhong, H., Boucher, O., Bréon, F. M., Lu, C., Guo, R., Xue, J., Boucher, E., … Chevallier, F. (2020). Carbon Monitor, a near-real-time daily dataset of global CO2 emission from fossil fuel and cement production. Scientific Data, 7(1). doi:10.1038/s41597-020-00708-7.

[2] Andrew, R. M. (2018). Global CO2 emissions from cement production. Earth System Science Data, 10(1), 195–217. doi:10.5194/essd-10-195-2018.

[3] Habert, G., Miller, S. A., John, V. M., Provis, J. L., Favier, A., Horvath, A., & Scrivener, K. L. (2020). Environmental impacts and decarbonization strategies in the cement and concrete industries. Nature Reviews Earth and Environment, 1(11), 559–573. doi:10.1038/s43017-020-0093-3.

[4] Kwasny, J., Aiken, T. A., Soutsos, M. N., McIntosh, J. A., & Cleland, D. J. (2018). Sulfate and acid resistance of lithomarge-based geopolymer mortars. Construction and Building Materials, 166, 537–553. doi:10.1016/j.conbuildmat.2018.01.129.

[5] Aiken, T. A., Kwasny, J., Sha, W., & Soutsos, M. N. (2018). Effect of slag content and activator dosage on the resistance of fly ash geopolymer binders to sulfuric acid attack. Cement and Concrete Research, 111, 23–40. doi:10.1016/j.cemconres.2018.06.011.

[6] Turner, L. K., & Collins, F. G. (2013). Carbon dioxide equivalent (CO2-e) emissions: A comparison between geopolymer and OPC cement concrete. Construction and Building Materials, 43, 125–130. doi:10.1016/j.conbuildmat.2013.01.023.

[7] Silva, P. De, Sagoe-Crenstil, K., & Sirivivatnanon, V. (2007). Kinetics of geopolymerization: Role of Al2O3 and SiO2. Cement and Concrete Research, 37(4), 512–518. doi:10.1016/j.cemconres.2007.01.003.

[8] Qu, F., Li, W., Wang, K., Zhang, S., & Sheng, D. (2021). Performance deterioration of fly ash/slag-based geopolymer composites subjected to coupled cyclic preloading and sulfuric acid attack. Journal of Cleaner Production, 321, 128942. doi:10.1016/j.jclepro.2021.128942.

[9] Dupuy, C., Havette, J., Gharzouni, A., Texier-Mandoki, N., Bourbon, X., & Rossignol, S. (2019). Metakaolin-based geopolymer: Formation of new phases influencing the setting time with the use of additives. Construction and Building Materials, 200, 272–281. doi:10.1016/j.conbuildmat.2018.12.114.

[10] Bayuaji, R., Nuruddin, M. F., Francis, S., Ekaputri, J. J., Triwulan, Junaedi, S., & Fansuri, H. (2015). Mechanical properties of MIRHA-fly ash geopolymer concrete. Materials Science Forum, 803, 49–57. doi:10.4028/www.scientific.net/MSF.803.49.

[11] Emoto, Y., Yoshizawa, K., Shikata, N., Tsubura, A., & Nagasaki, Y. (2016). Autopsy results of a case of ingestion of sodium hydroxide solution. Journal of Toxicologic Pathology, 29(1), 45–47. doi:10.1293/tox.2015-0049.

[12] Fujioka, M., Fukui, K., Yoshino, K., Noguchi, M., Soeda, M., & Ito, M. (2022). Microscopic changes over time in human dermis after exposure to sodium hydroxide. Burns Open, 6(2), 89–91. doi:10.1016/j.burnso.2022.03.002.

[13] Das, S. K., & Shrivastava, S. (2021). Influence of molarity and alkali mixture ratio on ambient temperature cured waste cement concrete based geopolymer mortar. Construction and Building Materials, 301, 124380. doi:10.1016/j.conbuildmat.2021.124380.

[14] Hajimohammadi, A., & van Deventer, J. S. J. (2017). Characterisation of One-Part Geopolymer Binders Made from Fly Ash. Waste and Biomass Valorization, 8(1), 225–233. doi:10.1007/s12649-016-9582-5.

[15] Liu, W., Zhao, J., Feng, Y., Zhang, B., & Xie, J. (2025). Seawater-mixed alkali-activated materials: A state-of-the-art review. Journal of Materials Science, 60(5), 2169-2198. doi:10.1007/s10853-025-10605-2.

[16] Askarian, M., Tao, Z., Adam, G., & Samali, B. (2018). Mechanical properties of ambient cured one-part hybrid OPC-geopolymer concrete. Construction and Building Materials, 186, 330–337. doi:10.1016/j.conbuildmat.2018.07.160.

[17] Petrus, H. T. B. M., Fairuz, F. I., Sa'dan, N., Olvianas, M., Astuti, W., Jenie, S. N. A., Setiawan, F. A., Anggara, F., Ekaputri, J. J., & Bendiyasa, I. M. (2021). Green geopolymer cement with dry activator from geothermal sludge and sodium hydroxide. Journal of Cleaner Production, 293(2), 126143. doi:10.1016/j.jclepro.2021.126143.

[18] Luukkonen, T., Abdollahnejad, Z., Yliniemi, J., Kinnunen, P., & Illikainen, M. (2018). One-part alkali-activated materials: A review. Cement and Concrete Research, 103(October), 21–34. doi:10.1016/j.cemconres.2017.10.001.

[19] Ma, C., Long, G., Shi, Y., & Xie, Y. (2018). Preparation of cleaner one-part geopolymer by investigating different types of commercial sodium metasilicate in China. Journal of Cleaner Production, 201, 636–647. doi:10.1016/j.jclepro.2018.08.060.

[20] Guo, S., Wu, Y., Jia, Z., Qi, X., & Wang, W. (2023). Sodium-based activators in alkali- activated materials: Classification and comparison. Journal of Building Engineering, 70(March), 106397. doi:10.1016/j.jobe.2023.106397.

[21] Olvianas, M., Najmina, M., Prihardana, B. S. L., Sutapa, F. A. K. G. P., Nurhayati, A., & Petrus, H. T. B. M. (2015). Study on the Geopolymerization of Geothermal Silica and Kaolinite. Advanced Materials Research, 1112, 528–532. doi:10.4028/www.scientific.net/amr.1112.528.

[22] Alcântara-Domingos, R. R., & Fungaro, D. A. (2025). Circular economy: development of calcium silicate hydrated compounds aimed at the sustainable use of waste from the coal industry. Brazilian Journal of Animal and Environmental Research, 8(1), e77647-e77647. doi:10.34188/bjaerv8n1-096.

[23] Khedmati, M., Alanazi, H., Kim, Y. R., Nsengiyumva, G., & Moussavi, S. (2018). Effects of Na2O/SiO2 molar ratio on properties of aggregate-paste interphase in fly ash-based geopolymer mixtures through multiscale measurements. Construction and Building Materials, 191, 564–574. doi:10.1016/j.conbuildmat.2018.10.024.

[24] Leonard Wijaya, A., Jaya Ekaputri, J., & Triwulan. (2017). Factors influencing strength and setting time of fly ash based-geopolymer paste. MATEC Web of Conferences, 138. doi:10.1051/matecconf/201713801010.

[25] Giergiczny, Z. (2019). Fly ash and slag. Cement and Concrete Research, 124(February). doi:10.1016/j.cemconres.2019.105826.

[26] Askarian, M., Tao, Z., Samali, B., Adam, G., & Shuaibu, R. (2019). Mix composition and characterisation of one-part geopolymers with different activators. Construction and Building Materials, 225, 526–537. doi:10.1016/j.conbuildmat.2019.07.083.

[27] Junaid, M. T., Khennane, A., Kayali, O., Sadaoui, A., Picard, D., & Fafard, M. (2014). Aspects of the deformational behaviour of alkali activated fly ash concrete at elevated temperatures. Cement and Concrete Research, 60, 24–29. doi:10.1016/j.cemconres.2014.01.026.

[28] Yousefi Oderji, S., Chen, B., Ahmad, M. R., & Shah, S. F. A. (2019). Fresh and hardened properties of one-part fly ash-based geopolymer binders cured at room temperature: Effect of slag and alkali activators. Journal of Cleaner Production, 225, 1–10. doi:10.1016/j.jclepro.2019.03.290.

[29] Dong, M., Elchalakani, M., & Karrech, A. (2020). Development of high strength one-part geopolymer mortar using sodium metasilicate. Construction and Building Materials, 236, 117611. doi:10.1016/j.conbuildmat.2019.117611.

[30] Triwulan, M., Ekaputri, J. J., & Priyanka, N. F. (2017). The Effect of Temperature Curing on Geopolymer Concrete. MATEC Web of Conferences, 97, 0–5. doi:10.1051/matecconf/20179701005.

[31] Ekaputri, J. J., Triwulan, Junaedi, S., Fansuri, & Aji, R. B. (2015). Light weight geopolymer paste made with Sidoarjo mud (Lusi). Materials Science Forum, 803, 63–74. doi:10.4028/www.scientific.net/MSF.803.63.

[32] L. Hake, S., Awasarmal, P. R., & Damgir, R. M. (2019). Durability Study on Fly Ash Based Geopolymer Concrete for Acidic Environment. Global Journal of Material Science and Engineering, August, 13–17. doi:10.37516/global.j.mater.sci.eng.2019.0076.

[33] Alnkaa, A., Yaprak, H., Memis, S., & Kaplan, G. (2018). Effect of Different Cure Conditions on the Shrinkage of Geopolymer Mortar Effect of Different Cure Conditions on the Shrinkage of Geopolymer Mortar. International Journal of Engineering Research and Development, 14(10), 51–55.

[34] Karim, M. R., Zain, M. F. M., Jamil, M., Lai, F. C., & Islam, M. N. (2011). Strength development of mortar and concrete containing fly ash: A review. International Journal of Physical Sciences, 6(17), 4137–4153. doi:10.5897/IJPS11.232.

[35] Cheerarot, R., & Jaturapitakkul, C. (2004). A study of disposed fly ash from landfill to replace Portland cement. Waste Management, 24(7), 701–709. doi:10.1016/j.wasman.2004.02.003.

[36] Aziz, I. H., Abdullah, M. M. A. B., Mohd Salleh, M. A. A., Azimi, E. A., Chaiprapa, J., & Sandu, A. V. (2020). Strength development of solely ground granulated blast furnace slag geopolymers. Construction and Building Materials, 250, 118720. doi:10.1016/j.conbuildmat.2020.118720.

[37] Swathi, B., & Vidjeapriya, R. (2023). Influence of precursor materials and molar ratios on normal, high, and ultra-high performance geopolymer concrete – A state of art review. Construction and Building Materials, 392, 132006. doi:10.1016/j.conbuildmat.2023.132006.

[38] Yaseri, S., Hajiaghaei, G., Mohammadi, F., Mahdikhani, M., & Farokhzad, R. (2017). The role of synthesis parameters on the workability, setting and strength properties of binary binder based geopolymer paste. Construction and Building Materials, 157, 534–545. doi:10.1016/j.conbuildmat.2017.09.102.

[39] Davidovits, J. (1991). Geopolymers - Inorganic polymeric new materials. Journal of Thermal Analysis, 37(8), 1633–1656. doi:10.1007/BF01912193.

[40] Wang, Y., Liu, X., Zhang, W., Li, Z., Zhang, Y., Li, Y., & Ren, Y. (2020). Effects of Si/Al ratio on the efflorescence and properties of fly ash based geopolymer. Journal of Cleaner Production, 244, 118852. doi:10.1016/j.jclepro.2019.118852.

[41] Lee, B., Kim, G., Kim, R., Cho, B., Lee, S., & Chon, C. M. (2017). Strength development properties of geopolymer paste and mortar with respect to amorphous Si/Al ratio of fly ash. Construction and Building Materials, 151, 512–519. doi:10.1016/j.conbuildmat.2017.06.078.

[42] de Jong, B. H. W. S., & Brown, G. E. (1980). Polymerization of silicate and aluminate tetrahedra in glasses, melts, and aqueous solutions-I. Electronic structure of H6Si2O7, H6AlSiO71-, and H6Al2O72-. Geochimica et Cosmochimica Acta, 44(3), 491–511. doi:10.1016/0016-7037(80)90046-0.

[43] Duxson, P., Provis, J. L., Lukey, G. C., Mallicoat, S. W., Kriven, W. M., & Van Deventer, J. S. J. (2005). Understanding the relationship between geopolymer composition, microstructure and mechanical properties. Colloids and Surfaces A: Physicochemical and Engineering Aspects, 269(1–3), 47–58. doi:10.1016/j.colsurfa.2005.06.060.

[44] Liu, J., Doh, J. H., Dinh, H. L., Ong, D. E. L., Zi, G., & You, I. (2022). Effect of Si/Al molar ratio on the strength behavior of geopolymer derived from various industrial waste: A current state of the art review. Construction and Building Materials, 329(February), 127134. doi:10.1016/j.conbuildmat.2022.127134.

[45] Liu, J., Li, X., Lu, Y., & Bai, X. (2020). Effects of Na/Al ratio on mechanical properties and microstructure of red mud-coal metakaolin geopolymer. Construction and Building Materials, 263, 120653. doi:10.1016/j.conbuildmat.2020.120653.

[46] Hou, L., Li, J., & Lu, Z. yuan. (2019). Effect of Na/Al on formation, structures and properties of metakaolin based Na-geopolymer. Construction and Building Materials, 226, 250–258. doi:10.1016/j.conbuildmat.2019.07.171.

[47] Provis, J. L., & van Deventer, J. S. J. (2007). Geopolymerisation kinetics. 2. Reaction kinetic modelling. Chemical Engineering Science, 62(9), 2318–2329. doi:10.1016/j.ces.2007.01.028.

[48] Rees, C. A., Provis, J. L., Lukey, G. C., & Van Deventer, J. S. J. (2007). In situ ATR-FTIR study of the early stages of fly ash geopolymer gel formation. Langmuir, 23(17), 9076–9082. doi:10.1021/la701185g.

[49] Ma, Z., Wang, W., Li, J., Gao, J., Lu, G., Song, H., Wu, H., & Guo, Y. (2023). Long-term dissolution behavior of amorphous aluminosilicate in sodium hydroxide solution for geopolymer synthesis using circulating fluidized bed combustion fly ash. Construction and Building Materials, 394 (August 2022), 132143. doi:10.1016/j.conbuildmat.2023.132143.

[50] Perdanawati, R. A., Risdanareni, P., Setiamarga, D. H. E., Ekaputri, J. J., Kusbiantoro, A., & Liao, M. C. (2024). The Potential of Seawater in Geopolymer Mixtures – Effect of Alkaline Activator, Seawater, and Steam Curing on the Strength of Geopolymer Paste. Journal of Ecological Engineering, 25(10), 370–380. doi:10.12911/22998993/192526.

[51] Jiao, Z., Li, X., & Yu, Q. (2021). Effect of curing conditions on freeze-thaw resistance of geopolymer mortars containing various calcium resources. Construction and Building Materials, 313(October), 125507. doi:10.1016/j.conbuildmat.2021.125507.

[52] Wu, H., He, M., Wu, S., Cheng, J., Wang, T., Che, Y., Du, Y., & Deng, Q. (2024). Effects of binder component and curing regime on compressive strength, capillary water absorption, shrinkage and pore structure of geopolymer mortars. Construction and Building Materials, 442(May), 137707. doi:10.1016/j.conbuildmat.2024.137707.

[53] Van Jaarsveld, J. G. S., Van Deventer, J. S. J., & Lukey, G. C. (2002). The effect of composition and temperature on the properties of fly ash- and kaolinite-based geopolymers. Chemical Engineering Journal, 89(1–3), 63–73. doi:10.1016/S1385-8947(02)00025-6.

[54] Saxena, S. K., & Kumar, M. (2018). Influence of alkali solutions on properties of pond fly ash-based geopolymer mortar cured under different conditions. Advances in Cement Research, 30(1), 1–7. doi:10.1680/jadcr.17.00038.

[55] Cheah, C. B., Tan, L. E., & Ramli, M. (2019). The engineering properties and microstructure of sodium carbonate activated fly ash/ slag blended mortars with silica fume. Composites Part B: Engineering, 160, 558–572. doi:10.1016/j.compositesb.2018.12.056.

[56] Lopes, A., Lopes, S., & Pinto, I. (2023). Influence of Curing Temperature on the Strength of a Metakaolin-Based Geopolymer. Materials, 16(23). doi:10.3390/ma16237460.

[57] Sajan, P., Jiang, T., Lau, C. K., Tan, G., & Ng, K. (2021). Combined effect of curing temperature, curing period and alkaline concentration on the mechanical properties of fly ash-based geopolymer. Cleaner Materials, 1(June), 100002. doi:10.1016/j.clema.2021.100002.

[58] Wu, R., Gu, Q., Gao, X., Huang, J., Guo, Y., & Zhang, H. (2024). Effect of curing conditions on the alkali-activated blends: Microstructure, performance and economic assessment. Journal of Cleaner Production, 445, 141344. doi:10.1016/j.jclepro.2024.141344.

[59] Petrus, H. T. B. M., Olvianas, M., Shafiyurrahman, M. F., Pratama, I. G. A. A. N., Jenie, S. N. A., Astuti, W., Nurpratama, M. I., Ekaputri, J. J., & Anggara, F. (2022). Circular Economy of Coal Fly Ash and Silica Geothermal for Green Geopolymer: Characteristic and Kinetic Study. Gels, 8(4). doi:10.3390/gels8040233.

[60] Liu, Z., Bu, L., Wang, Z., & Hu, G. (2019). Durability and microstructure of steam cured and autoclaved PHC pipe piles. Construction and Building Materials, 209, 679–689. doi:10.1016/j.conbuildmat.2019.03.166.

[61] Mustafa Al Bakri, A. M., Kamarudin, H., Bnhussain, M., Rafiza, A. R., & Zarina, Y. (2012). Effect of Na2SiO3/NaOH ratios and NaOH molarities on compressive strength of fly-ash-based geopolymer. ACI Materials Journal, 109(5), 503–508. doi:10.14359/51684080.

[62] Lv, X., Dong, Y., Wang, R., Lu, C., & Wang, X. (2020). Resistance improvement of cement mortar containing silica fume to external sulfate attacks at normal temperature. Construction and Building Materials, 258, 119630. doi:10.1016/j.conbuildmat.2020.119630.

[63] Zhang, S. S., Wang, S., Li, W., Cai, H., & Chen, X. (2025). Improving efflorescence resistance of metakaolin-based geopolymer via magnesium incorporation. Construction and Building Materials, 489, 142421. doi:10.1016/j.conbuildmat.2025.142421.

[64] Ge, Y., Tian, X., Huang, D., Zhong, Q., Yang, Y., & Peng, H. (2023). Understanding efflorescence behavior and compressive strength evolution of metakaolin-based geopolymer under a pore structure perspective. Journal of Building Engineering, 66(August 2022), 105828. doi:10.1016/j.jobe.2023.105828.

[65] Xu, Z., Yue, J., Pang, G., Li, R., Zhang, P., & Xu, S. (2021). Influence of the Activator Concentration and Solid/Liquid Ratio on the Strength and Shrinkage Characteristics of Alkali-Activated Slag Geopolymer Pastes. Advances in Civil Engineering, 2021. doi:10.1155/2021/6631316.

[66] Hanumananaik, M., & Subramaniam, K. V. L. (2023). Shrinkage in low-calcium fly ash geopolymers for precast applications: Reaction product content and pore structure under drying conditions. Journal of Building Engineering, 78, 107583. doi:10.1016/j.jobe.2023.107583.

[67] Ding, Y., Dai, J. G., & Shi, C. J. (2016). Mechanical properties of alkali-activated concrete: A state-of-the-art review. Construction and Building Materials, 127, 68–79. doi:10.1016/j.conbuildmat.2016.09.121.

[68] Zhang, H. Y., Kodur, V., Wu, B., Yan, J., & Yuan, Z. S. (2018). Effect of temperature on bond characteristics of geopolymer concrete. Construction and Building Materials, 163, 277–285. doi:10.1016/j.conbuildmat.2017.12.043.

[69] Zhang, H. Y., Liu, J. C., & Wu, B. (2021). Mechanical properties and reaction mechanism of one-part geopolymer mortars. Construction and Building Materials, 273. doi:10.1016/j.conbuildmat.2020.121973.

[70] Zhao, Q., Ma, C., Huang, B., & Lu, X. (2023). Development of alkali activated cementitious material from sewage sludge ash: Two-part and one-part geopolymer. Journal of Cleaner Production, 384, 135547. doi:10.1016/j.jclepro.2022.135547.

[71] Aliabdo, A. A., Abd Elmoaty, A. E. M., & Salem, H. A. (2016). Effect of water addition, plasticizer and alkaline solution constitution on fly ash based geopolymer concrete performance. Construction and Building Materials, 121, 694–703. doi:10.1016/j.conbuildmat.2016.06.062.

[72] Konduru, H., & Karthiyaini, S. (2024). Enhancing solidification in one-part geopolymer systems through alkali-thermal activation of bauxite residue and silica fume integration. Case Studies in Construction Materials, 21, 3444. doi:10.1016/j.cscm.2024.e03444.

[73] Ryu, G. S., Lee, Y. B., Koh, K. T., & Chung, Y. S. (2013). The mechanical properties of fly ash-based geopolymer concrete with alkaline activators. Construction and Building Materials, 47, 409–418. doi:10.1016/j.conbuildmat.2013.05.069.

[74] Chouksey, A., Verma, M., Dev, N., Rahman, I., & Upreti, K. (2022). An investigation on the effect of curing conditions on the mechanical and microstructural properties of the geopolymer concrete. Materials Research Express, 9(5), 055003. doi:10.1088/2053-1591/ac6be0.

[75] Chen, Z., Yu, J., Nong, Y., Yang, Y., Zhang, H., & Tang, Y. (2023). Beyond time: Enhancing corrosion resistance of geopolymer concrete and BFRP bars in seawater. Composite Structures, 322. doi:10.1016/j.compstruct.2023.117439.

[76] Zhang, M., Zhao, M., Zhang, G., Sietins, J. M., Granados-Focil, S., Pepi, M. S., Xu, Y., & Tao, M. (2018). Reaction kinetics of red mud-fly ash based geopolymers: Effects of curing temperature on chemical bonding, porosity, and mechanical strength. Cement and Concrete Composites, 93, 175–185. doi:10.1016/j.cemconcomp.2018.07.008.

[77] Christidis, G., Paipoutlidi, K., Marantos, I., & Perdikatsis, V. (2020). Determination of amorphous matter in industrial minerals with X-ray diffraction using Rietveld refinement. Bulletin of the Geological Society of Greece, 56(1), 1. doi:10.12681/bgsg.20940.

[78] Khale, D., & Chaudhary, R. (2007). Mechanism of geopolymerization and factors influencing its development: a review. Journal of materials science, 42(3), 729-746. doi:10.1007/s10853-006-0401-4.

[79] Wang, Y. S., Alrefaei, Y., & Dai, J. G. (2021). Roles of hybrid activators in improving the early-age properties of one-part geopolymer pastes. Construction and Building Materials, 306, 124880. doi:10.1016/j.conbuildmat.2021.124880.

[80] Ma, C., Zhao, B., Guo, S., Long, G., & Xie, Y. (2019). Properties and characterization of green one-part geopolymer activated by composite activators. Journal of Cleaner Production, 220, 188–199. doi:10.1016/j.jclepro.2019.02.159.

[81] Jaya Ekaputri, J., Syabrina Mutiara, I., Nurminarsih, S., Van Chanh, N., Maekawa, K., & Setiamarga, D. H. E. (2017). The effect of steam curing on chloride penetration in geopolymer concrete. MATEC Web of Conferences, 138. doi:10.1051/matecconf/201713801019.

[82] Al Bakri Abdullah, M. M., Mohd Tahir, M. F., Hussin, K., Binhussain, M., & Ekaputri, J. J. (2016). Effect of microwave curing to the compressive strength of fly ash based geopolymer mortar. Materials Science Forum, 841, 193–199. doi:10.4028/www.scientific.net/MSF.841.193.

[83] Zeyad, A. M., Tayeh, B. A., Adesina, A., de Azevedo, A. R. G., Amin, M., Hadzima-Nyarko, M., & Saad Agwa, I. (2022). Review on effect of steam curing on behavior of concrete. Cleaner Materials, 3. doi:10.1016/j.clema.2022.100042.